

Nonlinear modulation of dispersive fast magnetosonic waves in an inhomogeneous rotating solar low- β magnetoplasma

Jyoti Turi^{1,*} and A. P. Misra^{1,†}

¹*Department of Mathematics, Siksha Bhavana, Visva-Bharati University, Santiniketan-731 235, West Bengal, India*

(Dated: June 21, 2024)

We study the modulation of fast magnetosonic waves (MSWs) in rotating inhomogeneous low- β magnetoplasmas with the effects of gravitation and the Coriolis force. By employing the standard multiple-scale reductive perturbation technique (RPT), we derive a nonlinear Schrödinger (NLS) equation that governs the evolution of slowly varying MSW envelopes. The fast MSW becomes dispersive by the effects of the Coriolis force in the fluid motion, and the magnetic field and density inhomogeneity effects favor the Jeans instability in self-gravitating plasmas in a larger domain of the wave number (k , below the Jeans critical wave number, k_J) than homogeneous plasmas. The relative influence of the Jeans frequency (ω_J , associated with the gravitational force) and the angular frequency (Ω_0 , relating to the Coriolis force) on the Jeans carrier MSW mode and the modulational instability (MI) of the MSW envelope is studied. We show that the MSW envelope (corresponding to the unstable carrier Jeans mode with $\omega_J > 2\Omega_0$ and $k < k_J$) is always unstable against the plane wave perturbation with no cut-offs for growth rates. In contrast, the stable Jeans mode with $\omega_J > 2\Omega_0$ but $k > k_J$ manifests either modulational stability or MI having a finite growth rate before being cut off. We find an enhancement of the MI growth rate by the influence of magnetic field or density inhomogeneity. The case with constant gravity force (other than the self-gravity) perpendicular to the magnetic field is also briefly discussed to show that the fast magnetosonic carrier mode is always unstable, giving MI of slowly varying envelopes with no cut-offs for the growth rates. Possible applications of MI in solar plasmas, such as those in the X-ray corona, are also briefly discussed.

I. INTRODUCTION

One-fluid magnetohydrodynamics deals with a compressible conducting fluid immersed in a magnetic field and it is often regarded as a reasonable description of the large-scale dynamics of a plasma. Magnetohydrodynamic (MHD) waves are generally described applying this theory and represent one of the macroscopic processes responsible for the transformation of energy and information in plasmas. The theory of MHD waves in an infinite conducting medium was first developed by Alfvén [1] with its application to sunspots, coronal heating, particle acceleration, and generation of cosmic radiation. Since then, the study of nonlinear MHD waves in plasma has been one of the most popular research topics among researchers, given its remarkable application and progress in laboratory experiments and techniques as well as various space and astrophysical plasma environments like pulsar magnetosphere, magnetars, solar corona, etc.

Magnetosonic waves (MSWs) are one of the fundamental MHD wave modes in plasmas, which propagate nearly perpendicular to the background magnetic field and are often observed in laboratory plasmas [2], earth magnetosphere [3–7], and solar wind plasmas [8], etc. These waves are of great interest because of their important roles in plasma heating [9] and charged particle acceleration [10]. Several authors have investigated the characteristics of MSW waves in different space and astrophysical plasma environments. To mention a few, Marklund *et al.* [11]

studied the magnetosonic solitons in a quantum magnetoplasma, including the quantum Bohm potential and electron spin-1/2 effects using the Sagdeev potential approach. Haas and Mahmood [12] analyzed the propagation of linear and weakly nonlinear magnetosonic waves in a plasma with arbitrary degeneracy of electrons and with the inclusion of Bohm diffraction effects. Nonlinear properties of fast MSWs in dense dissipative plasmas with degenerate electrons were studied theoretically by Masood *et al.* [13] by deriving the Zabolotskaya-Khokhlov (ZK) equation for small but finite amplitude excitations. Hussain and Mahmood [14] investigated the nonlinear propagation of MSWs and showed that these waves may evolve into shock-like structures that may be responsible for heating the solar chromosphere and the solar corona.

The modulational instability (MI) of nonlinear waves in dispersive or diffractive media has been known to be one of the most important mechanisms of energy localization via the formation of different localized coherent structures like envelope solitons [15], envelope shocks [16], freak wave (or rouge waves) [17, 18], giant waves [19], etc., as well as the transfer of energy between waves and particles, leading to particle heating, e.g., heating of coronal loops [20]. In this context, Watanabe [21] first experimentally observed the MI of nonlinear wave envelopes in dispersive media in 1977. Subsequently, the investigations of MI and associated nonlinear structures have gained significant attention among researchers, and a large number of theoretical and experimental investigations on MI of electrostatic and electromagnetic waves have been done to explain the effects of different physical parameters in various space and astrophysical plas-

* jyotituri.maths@gmail.com

† apmisra@visva-bharati.ac.in

mas [22–25]. For example, Sahyouni *et al.* [26] studied the amplitude modulation of fast magnetosonic surface waves in solar flux tubes and showed that the fast wave-envelope admits dark envelope solitons solution and discussed the possibility of the existence of solitary waves in the solar atmosphere. Sakai [27] examined the MI of fast MSWs theoretically and discussed its applications to solar plasmas. Misra and Shukla [28] studied the MI of magnetosonic waves using a two-fluid quantum magnetohydrodynamic model that includes the effects of the electron-1/2 spin and the plasma resistivity. Panwar *et al.* have investigated the MI and associated rogue-wave structures of slow magnetosonic perturbations in a Hall-MHD plasma [29]. Wang *et al.* have studied the MI of MSWs in a Fermi-Dirac-Pauli plasma by the combined effects of the electron relativistic degeneracy, the quantum tunneling, electron spin via Pauli paramagnetism, and plasma resistivity [30].

To the best of our knowledge, the combined effects of the Coriolis force and the gravity force on the fast magnetosonic modes and the MI of slowly varying envelopes in inhomogeneous magnetoplasmas have not been studied before. Our aim is to study the propagation characteristics of fast magnetosonic modes and their nonlinear evolution as slowly varying envelopes through the modulational instability. To this end, we consider a self-consistent MHD model for electron and ion fluids that includes the combined effects of the gravity and Coriolis forces as well as the magnetic field and density inhomogeneities in absence of any viscosity or magnetic diffusivity. We show that while the fast magnetosonic modes exhibit instability in plasmas with constant gravity perpendicular to the magnetic field, the fast magnetosonic Jeans mode in self-gravitating plasmas can be stable or unstable depending on the competitive roles of the gravity and Coriolis forces and whether the Jeans wave number is below or above a critical value. The possibility of the emergence of MI of slowly varying magnetosonic envelopes in different cases of the stable or unstable fast carrier modes in presence of the self-gravitation and the constant gravity force with the effects of magnetic field or density inhomogeneities are studied and its applications to solar coronal plasmas are discussed.

The paper is organised in the following fashion: In Sec. II, we present the basic MHD models governing the dynamics of fast magnetosonic waves and the inhomogeneous equilibrium state of plasmas. Section III demonstrate the linear fast magnetosonic mode, the compatibility condition, and the derivation of the nonlinear Schrödinger (NLS) equation for the evolution of slowly varying magnetosonic envelopes. We study the MI in Sec. IV for three different cases of stable and unstable Jeans carrier modes as well as for the unstable carrier mode under the influence of gravity. The applications of our results in solar plasmas are discussed in Sec. V. Finally, Sec. VI is left to summarize and conclude our results.

II. BASIC EQUATIONS

We consider the nonlinear propagation of fast magnetosonic waves in a rotating magnetized plasma with the effects of the Coriolis force and the gravitational force. The latter may be considered in two cases (i) when the gravitational acceleration g is not a constant (self-gravity) and (ii) when g is a constant. The plasma is supposed to be rotating with uniform angular velocity $\boldsymbol{\Omega} = (0, \Omega_0 \cos \lambda, \Omega_0 \sin \lambda)$ and immersed in an external static magnetic field along the z -axis, i.e. $\mathbf{B}_0 = B_0 \hat{z}$. We assume the gravitational force to be acting vertically downwards and perpendicular to the magnetic field and the wave propagation along the x -axis, for simplicity. Furthermore, the background magnetic field and the density are assumed to vary along the x -axis (inhomogeneities). A schematic diagram for the model is shown in Fig. 1. We first consider the case of self-gravitating plasmas. The basic equations describing the dynamics of electron-ion fluids in self-gravitating magnetoplasmas in the center-of-mass frame are [31]

$$\frac{\partial \rho}{\partial t} + \nabla \cdot (\rho \mathbf{v}) = 0, \quad (1)$$

$$\frac{\partial \mathbf{v}}{\partial t} + (\mathbf{v} \cdot \nabla) \mathbf{v} = -\frac{1}{\rho} \nabla \left(P + \frac{\mathbf{B}^2}{2\mu_0} \right) + \frac{1}{\rho\mu_0} (\mathbf{B} \cdot \nabla) \mathbf{B} - 2\boldsymbol{\Omega} \times \mathbf{v} + \mathbf{g}, \quad (2)$$

$$\frac{\partial \mathbf{B}}{\partial t} + (\mathbf{v} \cdot \nabla) \mathbf{B} = (\mathbf{B} \cdot \nabla) \mathbf{v} - (\nabla \cdot \mathbf{v}) \mathbf{B}, \quad (3)$$

$$\nabla \cdot \mathbf{g} = -4\pi G\rho, \quad (4)$$

where $\mathbf{g} = -\nabla\psi$ is the gravitational force per unit mass of the fluid acting vertically downwards; ρ , \mathbf{v} , and P are, respectively, the fluid density, fluid velocity, and the thermal pressure. Also, \mathbf{B} , $\boldsymbol{\Omega}$, ψ , and G , respectively, denote the magnetic field, uniform angular velocity of the rotating fluid, gravitational potential, and the universal gravitational constant. The pressure P satisfies the equation of state: $\nabla P = c_s^2 \nabla \rho$, where $c_s = \sqrt{\gamma k_B T_e / m_i}$ is the adiabatic sound speed with k_B denoting the Boltzmann constant, T_e the electron temperature, γ the adiabatic index, and m_i the ion mass.

Next, we consider the one-dimensional propagation of fast MSWs along the x -axis and normalize Eqs. (1)-(4) according to: $\rho \rightarrow \rho/\rho_0$, $B \rightarrow B/B_0$, $\omega \rightarrow \omega/\omega_{ci}$, $(v_x, v_y, v_z) \rightarrow (v_x, v_y, v_z)/V_A$, $c_s \rightarrow c_s/V_A$, $\Omega_0 \rightarrow \Omega_0/\omega_{ci}$, $\omega_J \rightarrow \omega_J/\omega_{ci}$, $\psi \rightarrow \psi/V_A^2$. Here, $V_A = B_0/\sqrt{\mu_0\rho_0}$ is the Alfvén speed, $\omega_J^2 = 4\pi G\rho_0$ is the squared Jeans frequency, and $\omega_{ci} = \sqrt{eB_0/m_i}$ is the ion-cyclotron frequency at $x = 0$. Furthermore, the space and time coordinates are normalized as $x \rightarrow x\omega_{ci}/V_A$ and $t \rightarrow t\omega_{ci}$. Thus, from Eqs. (1)-(4), after separating the velocity components along the axes and noting

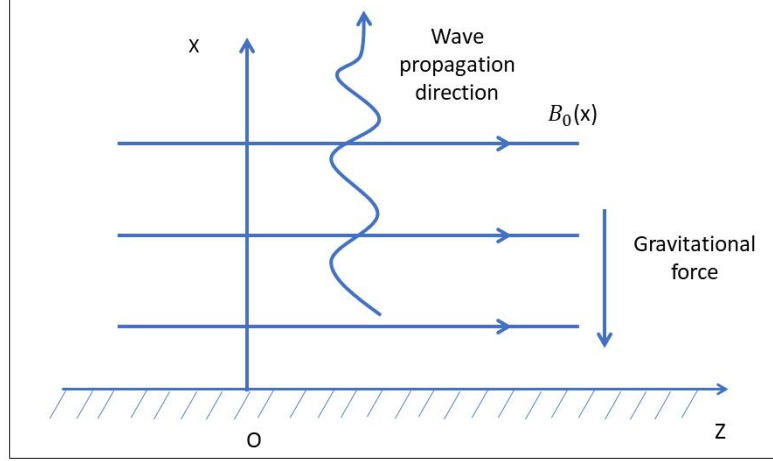


FIG. 1. A schematic diagram showing the directions of wave propagation \mathbf{k} , the external magnetic field \mathbf{B}_0 , and the gravitational force \mathbf{g} . The background plasma state is determined by Eqs. (10), (11). The magnetic field and density inhomogeneities are along the x -axis.

that the frozen-in-field condition $\rho/\rho_0 = B/B_0$ holds for Eqs. (1) and (3), we obtain the following reduced set of normalized equations

$$\frac{\partial B}{\partial t} + \frac{\partial}{\partial x}(v_x B) = 0, \quad (5)$$

$$\begin{aligned} \frac{\partial v_x}{\partial t} + v_x \frac{\partial v_x}{\partial x} &= -c_s^2 \frac{1}{B} \frac{\partial B}{\partial x} - \frac{1}{2} \frac{1}{B} \frac{\partial B^2}{\partial x} \\ &- 2(\Omega_0 v_z \cos \lambda - \Omega_0 v_y \sin \lambda) + \frac{\partial \psi}{\partial x}, \end{aligned} \quad (6)$$

$$\frac{\partial v_y}{\partial t} + v_x \frac{\partial v_y}{\partial x} = -2\Omega_0 v_x \sin \lambda, \quad (7)$$

$$\frac{\partial v_z}{\partial t} + v_x \frac{\partial v_z}{\partial x} = 2\Omega_0 v_x \cos \lambda, \quad (8)$$

$$\frac{\partial^2 \psi}{\partial x^2} + \omega_J^2 B = 0. \quad (9)$$

A. Equilibrium state

At equilibrium, the background plasma state with density and magnetic field inhomogeneities is defined by the following pressure-balance and the Poisson equations

$$\frac{d}{dx} \left(P_0(x) + \frac{B_0^2(x)}{2\mu_0} \right) = -\rho_0(x) \frac{d\psi_0(x)}{dx}, \quad (10)$$

$$\frac{d^2 \psi_0(x)}{dx^2} = 4\pi G \rho_0(x), \quad (11)$$

where the suffix ‘0’ denotes the equilibrium value of the corresponding physical quantity. We define $B_0(0) = B_0$, $\rho_0(0) = \rho_0$ and $\psi_0(0) = \psi_0$. By means of the normalization defined before, Eqs. (10) and (11) reduce to

$$\frac{d}{dx} \left(c_s^2 \rho_0(x) + \frac{1}{2} B_0^2(x) \right) = -\rho_0(x) \frac{d\psi_0(x)}{dx}, \quad (12)$$

$$\frac{d^2 \psi_0(x)}{dx^2} = \omega_J^2 \rho_0(x). \quad (13)$$

Using the relation $\nabla P = c_s^2 \nabla \rho$, and noting that $B_0(x)/B_0 = \rho_0(x)/\rho_0$ (Frozen-in-field condition), we obtain from Eq. (12), the following relation (in normalized form)

$$c_s^2 \ln \rho_0(x) + 2\rho_0(x) = \tilde{\psi}_0 - \psi_0(x), \quad (14)$$

where $\tilde{\psi}_0 = 2 + \psi_0$. Typically, if $\rho_0(x)$ is not too small, i.e., if it lies in $0.5 \lesssim \rho_0(x) \lesssim 1$, the function $\ln \rho_0(x)/\rho_0(x)$ approaches from small negative values to zero as $\rho_0(x) \rightarrow 1$. In addition, if the magnetic force dominates over the pressure gradient force (in low- β plasmas such as those in solar corona) or if the length scale of magnetic field inhomogeneity is much smaller than the density inhomogeneity, i.e., $L_{B_0} \ll L_{\rho_0}$, where $1/L_{\rho_0} \equiv [1/\rho_0(x)](d\rho_0(x)/dx)$ and $1/L_{B_0} \equiv [1/B_0(x)](dB_0(x)/dx)$, then the term proportional to c_s^2 in Eq. (14) can be neglected compared to the term involving the factor 2 (the second term on the left-hand side). Thus, from Eqs. (13) and (14), we obtain for $x > 0$ the following approximate solutions for $\psi_0(x)$ and $\rho_0(x)$.

$$\begin{aligned} \psi_0(x) &\approx \tilde{\psi}_0 - 2 \exp\left(-\frac{1}{2} \omega_J^2 x\right), \\ \rho_0(x) \equiv B_0(x) &\approx \frac{1}{2} \left[\tilde{\psi}_0 - \psi_0(x) \right]. \end{aligned} \quad (15)$$

On the other hand, if the contribution from the pressure gradient force is much higher than the magnetic force (in high- β plasmas such as those in the solar photosphere and solar wind acceleration region) or if the length scale of magnetic field inhomogeneity is much larger than the density inhomogeneity, i.e., $L_{B_0} \gg L_{\rho_0}$, approximate solutions for $\rho_0(x)$ and $\psi_0(x)$ can then be obtained from Eqs. (13) and (14) as ($x > 0$)

$$\begin{aligned} \psi_0(x) &\approx c_s^2 \left[1 - \bar{\psi}_0 \exp \left(-\frac{\omega_J^2}{c_s^2} x \right) \right], \\ \rho_0(x) \equiv B_0(x) &\approx \exp \left(\frac{\psi_0 - \psi_0(x)}{c_s^2} \right), \end{aligned} \quad (16)$$

where $\bar{\psi}_0 = 1 - \psi_0/c_s^2$. Furthermore, for plasmas where the plasma pressure is comparable to the magnetic pressure ($\beta \sim 1$), such as those in the lower chromospheric region of the solar atmosphere, Eqs. (13) and (14) are to be solved numerically. However, we are not considering these two cases in the present investigation.

III. DERIVATION OF NLS EQUATION

We study the modulation of weakly nonlinear slowly varying magnetosonic wave envelopes that are generated due to nonlinear self-interactions of carrier fast magnetosonic modes and higher harmonic modes in self-gravitating rotating magnetoplasmas. To this end, we employ the standard multiple-scale reductive perturbation technique (RPT) [32] to Eqs. (5)-(9) and derive the nonlinear Schrödinger equation for the evolution of slowly varying MSW envelopes. In the RPT, we define a new frame of reference in which the space and time variables are stretched as

$$\begin{aligned} \xi &= \epsilon(x - v_g t), \\ \tau &= \epsilon^2 t, \end{aligned} \quad (17)$$

where v_g is the group velocity of the wave envelope along the x -axis and ϵ is a small ($0 < \epsilon \ll 1$) expansion parameter, which scales the weakness of amplitudes of perturbations. Due to the stretched coordinates (17), the space and time derivatives will be replaced according to the following transformations.

$$\begin{aligned} \frac{\partial}{\partial t} &\rightarrow \frac{\partial}{\partial t} - \epsilon v_g \frac{\partial}{\partial \xi} + \epsilon^2 \frac{\partial}{\partial \tau}, \\ \frac{\partial}{\partial x} &\rightarrow \frac{\partial}{\partial x} + \epsilon \frac{\partial}{\partial \xi}, \\ \frac{\partial^2}{\partial x^2} &\rightarrow \frac{\partial^2}{\partial x^2} + 2\epsilon \frac{\partial^2}{\partial x \partial \xi} + \epsilon^2 \frac{\partial^2}{\partial \xi^2}. \end{aligned} \quad (18)$$

The dynamical variables are divided into unperturbed (equilibrium) and perturbed parts. In the latter, the slow and fast scales (for space and time), respectively, enter the l -th harmonic amplitudes and the phase ($kx - \omega t$).

Thus, the variables can be expanded as

$$\begin{aligned} B &= B_0(x) + \sum_{n=1}^{\infty} \epsilon^n \sum_{l=-\infty}^{\infty} B_l^{(n)}(\xi, \tau) \exp [il(kx - \omega t)], \\ v_x &= 0 + \sum_{n=1}^{\infty} \epsilon^n \sum_{l=-\infty}^{\infty} v_{xl}^{(n)}(\xi, \tau) \exp [il(kx - \omega t)], \\ v_y &= 0 + \sum_{n=1}^{\infty} \epsilon^n \sum_{l=-\infty}^{\infty} v_{yl}^{(n)}(\xi, \tau) \exp [il(kx - \omega t)], \\ v_z &= 0 + \sum_{n=1}^{\infty} \epsilon^n \sum_{l=-\infty}^{\infty} v_{zl}^{(n)}(\xi, \tau) \exp [il(kx - \omega t)], \\ \psi &= \psi_0(x) + \sum_{n=1}^{\infty} \epsilon^n \sum_{l=-\infty}^{\infty} \psi_l^{(n)}(\xi, \tau) \exp [il(kx - \omega t)], \end{aligned} \quad (19)$$

where $B_0(x)$ and $\psi_0(x)$ are normalized by B_0 and ψ_0 respectively, and the slowly varying wave amplitudes $B_l^{(n)}$, $v_{xl}^{(n)}$, $v_{yl}^{(n)}$, $v_{zl}^{(n)}$, $\psi_l^{(n)}$, etc. satisfy the reality condition: $A_{-l}^{(n)} = A_l^{(n)*}$, where the asterisk denotes the complex conjugate, and k and ω are, respectively, the wave number and the wave frequency of fast carrier MSWs.

In what follows, we apply the transformations [Eqs. (17) and (18)] and substitute the expansions [Eq. (19)] into the normalized Eqs. (5)-(9), and then obtain equations for different harmonic modes corresponding to different powers of ϵ (For some details, see Appendix VI). Here, we assume that the length scales of the density (L_{ρ_0}) and magnetic field (L_{B_0}) inhomogeneities are much larger than the length scale (L) of magnetosonic perturbations, i.e., $L_{\rho_0}, L_{B_0} \gg L$. With these assumptions, the imaginary contributions originating from the inhomogeneities can be ignored. The results are given in Secs. III A-III C.

A. First-order perturbations: Linear dispersion relation

For the first-order first harmonic perturbations, we obtain from the coefficients of ϵ , the following relations

$$v_{x1}^{(1)} = \frac{\omega}{k} B_1^{(1)}, \quad v_{y1}^{(1)} = -i \frac{2}{k} \Omega_0 \sin \lambda B_1^{(1)}, \quad (20)$$

$$\begin{aligned} v_{z1}^{(1)} &= i \frac{2}{k} \Omega_0 \cos \lambda B_1^{(1)}, \quad \psi_1^{(1)} = \frac{\omega_J^2}{k^2} B_1^{(1)}, \\ &- i \omega v_{x1}^{(1)} + ik(c_s^2 + V_A(x)^2) B_1^{(1)} \\ &+ 2\Omega_0 \left(\cos \lambda v_{z1}^{(1)} - \sin \lambda v_{y1}^{(1)} \right) - ik\psi^{(1)} = 0, \end{aligned} \quad (21)$$

where $V_A(x) = B_0(x)/\sqrt{\mu_0 \rho_0(x)}$ is the normalized inhomogeneous Alfvén velocity.

Next, eliminating the variables and looking for their nonzero solutions, we obtain from Eqs. (20)-(21), the

following linear dispersion relation for the fast carrier magnetosonic modes in self-gravitating magnetoplasmas.

$$\begin{aligned} \omega^2 &= [c_s^2 + V_A^2(x)] k^2 + 4\Omega_0^2 - \omega_J^2, \\ \text{i.e., } \omega &= [c_s^2 + V_A^2(x)]^{1/2} (k^2 - k_J^2)^{1/2}, \end{aligned} \quad (22)$$

where k_J is the critical Jeans wave number modified by the Coriolis force, given by,

$$k_J = \left(\frac{\omega_J^2 - 4\Omega_0^2}{c_s^2 + V_A^2(x)} \right)^{1/2}. \quad (23)$$

From Eq. (22), we note that the fast magnetosonic wave becomes dispersive due to the presence of the term proportional to Ω_0^2 , associated with the Coriolis force, and the Jeans instability may occur due to the term proportional to ω_J^2 by the influence of the self-gravitating force [33]. The instability occurs in the region $k < k_J$, provided the self-gravity force dominates over the Coriolis force, i.e., $\omega_J > 2\Omega_0$. In the other region, i.e., $k > k_J$, the magnetosonic wave can propagate as a real (stable) eigenmode with $\omega_J > 2\Omega_0$. On the other hand, in absence of the gravity effects or when the Coriolis force dominates over the self-gravity force with $\omega_J < 2\Omega_0$, the MSWs can also propagate as a real mode (without any instability) with the frequency being smaller or larger than the ion-cyclotron frequency and the dispersion relation in the form of high-frequency Langmuir waves in classical plasmas. Thus, it is reasonable to investigate the nonlinear modulation of slowly varying magnetosonic fields by means of a NLS equation. We also note that the effects of the magnetic field and the density inhomogeneities enter the coefficient of k^2 via the Alfvén velocity $V_A(x)$, implying that the wave dispersion is greatly modified by the effects of inhomogeneities, and hence the modifications of the phase velocity as well as the group velocity dispersion of magnetosonic envelopes.

Figure 2 displays the profiles of the real wave mode ($\Re\omega$, for $k > k_J$) and the growth rate of instability ($\Im\omega$, for $k < k_J$) by the effects of the density and magnetic field inhomogeneities [See Eq. (15)], the Coriolis force, and the self-gravity force such that $\omega_J > 2\Omega_0$. We find that while the real wave frequency increases with the wave number k , the instability growth rate falls off from a nonzero value with k having a cut-off at the critical Jeans wave number, i.e., $k = k_J$. Such a critical value shifts towards a higher value of k due to the effects of the inhomogeneities in which $\psi_0(x)$ increases, but $\rho_0(x)$ decreases with increasing values of $x > 0$. In this case, the instability domain for k expands and the domain of the real wave mode reduces. Thus, it follows that the density and magnetic field inhomogeneities in the background plasma favor the Jeans instability in a wide range of values of k , not reported before. On the other hand, a small reduction of the angular frequency Ω_0 of the rotating fluid, associated with the Coriolis force, can significantly

reduce both the growth rate of instability and the instability domain in k . We do not consider the case of $\omega_J \approx 2\Omega_0$ at which the fast magnetosonic wave becomes dispersionless. Such a strict condition may be applicable to low-frequency long-wavelength plasma oscillations.

B. Second-order perturbations: Compatibility condition

For the second order ($n = 2$) reduced equations with $l = 1$, we obtain the following expressions for different harmonic modes

$$\begin{aligned} v_{x1}^{(2)} &= \frac{\omega}{k} B_1^{(2)} - \frac{i(v_g k - \omega)}{k^2} \frac{\partial B_1^{(1)}}{\partial \xi}, \\ v_{y1}^{(2)} &= -\frac{2i\Omega_0 \sin \lambda}{k} B_1^{(2)} + \frac{2\Omega_0 \sin \lambda}{k^2} \frac{\partial B_1^{(1)}}{\partial \xi}, \\ v_{z1}^{(2)} &= \frac{2i\Omega_0 \cos \lambda}{k} B_1^{(2)} - \frac{2\Omega_0 \cos \lambda}{k^2} \frac{\partial B_1^{(1)}}{\partial \xi}, \\ \psi_1^{(2)} &= \frac{\omega_J^2}{k^2} B_1^{(2)} + \frac{2i\omega_J^2}{k^3} \frac{\partial B_1^{(1)}}{\partial \xi}, \end{aligned} \quad (24)$$

together with the compatibility condition

$$v_g \equiv \frac{\partial \omega}{\partial k} = [c_s^2 + V_A^2(x)]/v_p, \quad (25)$$

where $v_p = \omega/k$ is the phase velocity of the carrier magnetosonic waves. From Eq. (25), it is evident that the group velocity v_g of the wave envelope has an inverse relationship with the phase velocity of the carrier wave, i.e., the magnitude of the group velocity increases with a reduction of the magnitude of the phase velocity. Because of the dependency of v_g on the wave frequency ω , the group velocity can be real (imaginary) for $k > k_J$ ($k < k_J$) when $\omega_J > 2\Omega_0$. It can also be real when $\omega_J < 2\Omega_0$ for any real value of k . The expression for v_g is clearly modified by the effects of the background magnetic field or density inhomogeneity. Furthermore, having known the characteristics of ω (See Fig. 2), one can also investigate the features of the real and imaginary parts of v_g . It is seen that the real part of the group velocity decreases with $k > k_J$ and it can be further reduced (increased) by the effects of the density or magnetic field inhomogeneity (Coriolis force). On the other hand, the imaginary part of v_g is always negative in the domain $k < k_J$ and its magnitude increases with increasing values of k . The detailed analysis of v_g is not necessary at this stage, we will rather focus on the coefficients of the NLS equation to be derived in Sec. III C.

C. Third-order perturbations: The NLS equation

The second-order harmonic modes for $n = 2$ and $l = 2$ appear due to the nonlinear self-interaction of the carrier waves, and they are found to be proportional to $[B_1^1]^2$ as

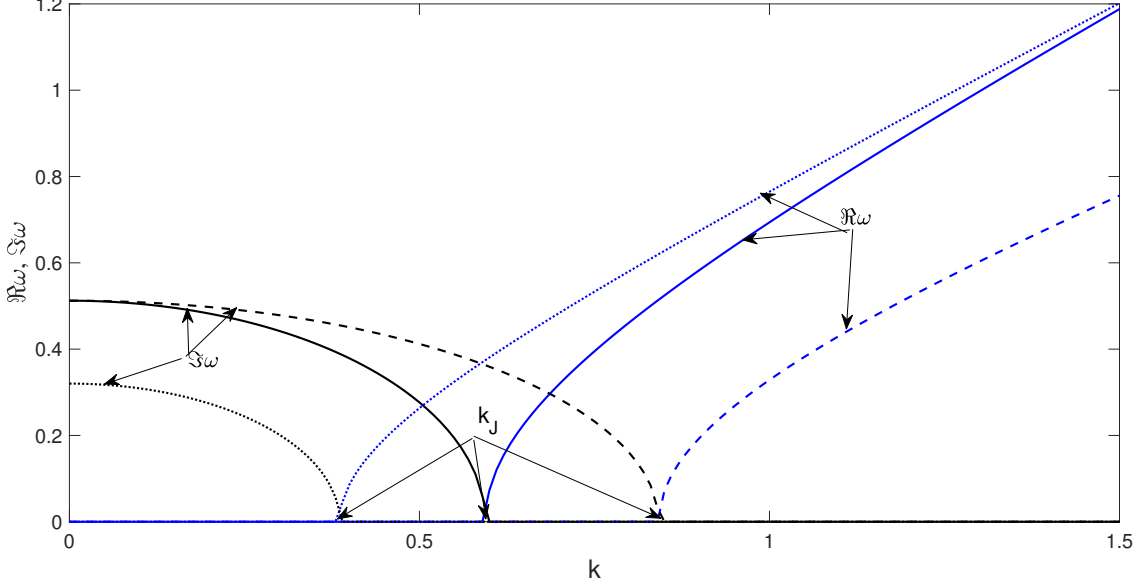


FIG. 2. The real ($\Re\omega$) and imaginary ($\Im\omega$) parts of the fast magnetosonic wave frequency ω [Eq. (22)] are shown when $\omega_J > 2\Omega_0$. The solid, dashed, and dotted lines correspond to the parameter values (i) $\Omega_0 = 0.8$, $\omega_J = 2.1\Omega_0$, $x = 0.5$, (ii) $\Omega_0 = 0.8$, $\omega_J = 2.1\Omega_0$, $x = 1.5$, and (iii) $\Omega_0 = 0.5$, $\omega_J = 2.1\Omega_0$, $x = 1.5$ respectively. The other fixed parameter values are $c_s = 0.5$ and $\psi_0 = -0.5$.

$$\begin{aligned}
 v_{x_2}^{(2)} &= \frac{\omega}{k} B_2^{(2)} - \frac{\omega}{k} [B_1^{(1)}]^2, \\
 v_{y_2}^{(2)} &= -\frac{i\Omega_0 \sin \lambda}{k} \frac{2}{3(4\Omega_0^2 - \omega_J^2)} [\{2c_s^2 + 3V_A^2(x)\}k^2 + 12\Omega_0^2 - 3\omega_J^2] [B_1^{(1)}]^2, \\
 v_{z_2}^{(2)} &= \frac{i\Omega_0 \cos \lambda}{k} \frac{2}{3(4\Omega_0^2 - \omega_J^2)} [\{2c_s^2 + 3V_A^2(x)\}k^2 + 12\Omega_0^2 - 3\omega_J^2] [B_1^{(1)}]^2, \\
 \psi_2^{(2)} &= \frac{\omega_J^2}{4k^2} \frac{2}{3(4\Omega_0^2 - \omega_J^2)} [\{2c_s^2 + 3V_A^2(x)\}k^2 + 12\Omega_0^2 - 3\omega_J^2] [B_1^{(1)}]^2, \\
 B_2^{(2)} &= \frac{2}{3(4\Omega_0^2 - \omega_J^2)} [\{2c_s^2 + 3V_A^2(x)\}k^2 + 12\Omega_0^2 - 3\omega_J^2] [B_1^{(1)}]^2.
 \end{aligned} \tag{26}$$

The nonlinear self-interactions of the first-order carrier wave modes also result into the generation of the zeroth harmonic modes. Thus, for $n = 2$, $l = 0$ we obtain

$$\begin{aligned}
 B_0^{(2)} &= v_{y_0}^{(2)} = v_{z_0}^{(2)} = 0, \\
 v_{x_0}^{(2)} &= -\frac{2\omega}{k} |B_1^{(1)}|^2, \\
 \psi_0^{(2)} &= \frac{(2\omega^2 + k^2 - 4\Omega_0^2)}{k^2} |B_1^{(1)}|^2.
 \end{aligned} \tag{27}$$

Finally, substituting all the above derived expressions into the third-order harmonic modes ($n = 3$ and $l = 1$), we obtain the following NLS equation

$$i \frac{\partial B}{\partial \tau} + P \frac{\partial^2 B}{\partial \xi^2} + Q |B|^2 B = 0, \tag{28}$$

where we have replaced $B_1^{(1)}$ by B for simplicity. The group velocity dispersion coefficient P and the nonlin-

ear coefficient Q , appeared due to the carrier wave self-interactions, are given by

$$\begin{aligned}
 P &\equiv \frac{1}{2} \frac{\partial^2 \omega}{\partial k^2} = \frac{1}{2} \frac{(c_s^2 + V_A^2(x))}{\omega^3} (4\Omega_0^2 - \omega_J^2) \\
 &= \frac{1}{2} \frac{4\Omega_0^2 - \omega_J^2}{[c_s^2 + V_A^2(x)]^{1/2} (k^2 - k_J^2)^{3/2}},
 \end{aligned} \tag{29}$$

$$\begin{aligned}
 Q &= \frac{1}{2\omega} \left[\omega^2 - \frac{2}{3} \frac{(3\omega^2 - c_s^2 k^2)}{(4\Omega_0^2 - \omega_J^2)} \right. \\
 &\quad \left. \times \left\{ (2\omega^2 + k^2) - \frac{1}{2} (4\Omega_0^2 - \omega_J^2) \right\} \right].
 \end{aligned} \tag{30}$$

From the dispersion Eq. (22), we note that the wave frequency ω can be either real or purely imaginary depending on whether $k > k_J$ or $k < k_J$. So, the coefficients P and Q can also be either real or purely imaginary. While the coefficient P appears due to the group

velocity dispersion and the coupling of the thermal and magnetic pressures with the Coriolis and the Gravity forces, the coefficient Q appears due to the nonlinear self-interactions of higher harmonic modes and coupling between the zeroth- and second-order second harmonic carrier waves. Specifically, the first term of Q appears due to transverse velocity perturbations and the second term of Q is due to the coupling between the zeroth and second harmonic modes. Before proceeding to study the modulational instability and the evolution of magnetosonic wave envelopes, it is pertinent to mention there cases of interest:

- Case I: $\omega_J < 2\Omega_0, \forall k$.
- Case II: $\omega_J > 2\Omega_0, k > k_J$.
- Case III: $\omega_J > 2\Omega_0, k < k_J$.

From the linear analysis in Sec. III A, we have noted that while Cases I and II correspond to the Jeans stable mode, Case III corresponds to the Jeans instability. Thus, it is of interest to study the modulational instability conditions in these three cases. Specifically, we will examine whether the Jeans instability region of carrier waves can give rise to the modulational instability of magnetosonic envelopes.

IV. MODULATIONAL INSTABILITY

We follow a similar technique as in [34] to study the modulation of magnetosonic wave envelopes against a plane wave perturbation. Though the analysis is standard, we reproduce it here for the sake of clarity to the readers. The NLS Eq. (28) admits a plane wave time-dependent solution of the form

$$B = \eta^{1/2} \exp\left(i \int_a^\xi \frac{\sigma}{2P} d\xi\right), \quad (31)$$

where a is some constant, and η and σ are real functions of ξ and τ . Substituting Eq. (31) into Eq. (28), and separating the real and imaginary parts, we obtain

$$\frac{\partial \eta}{\partial \tau} + \frac{\partial(\eta\sigma)}{\partial \xi} = 0, \quad (32)$$

$$\begin{aligned} \frac{\partial \sigma}{\partial \tau} + \sigma \frac{\partial \eta}{\partial \xi} = & 2PQ \frac{\partial \eta}{\partial \xi} \\ & + P^2 \frac{\partial}{\partial \xi} \left[\eta^{-1/2} \frac{\partial}{\partial \xi} \left(\eta^{-1/2} \frac{\partial \eta}{\partial \xi} \right) \right]. \end{aligned} \quad (33)$$

Next, we modulate the wave amplitude and phase by small plane-wave perturbations with the wave number K and the wave frequency Ω as

$$\begin{aligned} \eta &= \eta_0 + \eta_1 \cos(K\xi - \Omega\tau) + \eta_2 \sin(K\xi - \Omega\tau), \\ \sigma &= \sigma_1 \cos(K\xi - \Omega\tau) + \sigma_2 \sin(K\xi - \Omega\tau), \end{aligned} \quad (34)$$

where η_0 is a constant, and η_j and σ_j for $j = 1, 2$, are the amplitudes of perturbations.

Substituting the perturbation expansion (34) in Eqs. (32) and (33), and looking for nonzero solutions of η_1 and η_2 , we obtain the following dispersion relation for the perturbed wave of modulation in self-gravitating rotating magnetoplasmas

$$\Omega^2 = P^2 K^2 \left(K^2 - \frac{2\eta_0 Q}{P} \right). \quad (35)$$

In Subsections IV A-IV C, we will study the conditions for the modulational instability and the instability growth rate in the three different cases as mentioned above.

A. Case I: $\omega_J < 2\Omega_0, \forall k$

We consider the case when the contribution from the Coriolis force dominates over the self-gravitating force, i.e. when $\omega_J < 2\Omega_0$. In this case, the carrier Jeans wave frequency ω becomes real for any values of the wave number k [See Eq. (22)], and so are P and Q . Also, from Eq. (29), it is evident that that $P > 0$ for $\omega_J < 2\Omega_0$. Furthermore, inspecting on the expression of Q [Eq. (30)], we find that when $\omega_J < 2\Omega_0$ holds, the second term of Q becomes positive and larger than the first term, giving $Q < 0$. Thus, in this case, $PQ < 0$, and Eq. (35) gives a real wave frequency Ω for the perturbation of modulation, implying that the slowly varying magnetosonic wave envelope is always stable under the modulation. It follows that the modulated magnetosonic wave is also stable in absence of the self-gravity force.

B. Case II: $\omega_J > 2\Omega_0, k > k_J$

We consider the case when the self-gravitating force dominates over the Coriolis force, i.e. $\omega_J > 2\Omega_0$ and $k > k_J$. In this case, as discussed before in Sec. III A, since the carrier wave frequency ω is real, the coefficients P and Q of the NLS equation are also real. However, in contrast to Case I, $P < 0$ and Q can be both positive and negative for $k (> k_J)$, so that one can have both stable ($PQ < 0$) and unstable ($PQ > 0$) regions. Figure 3 shows the plot of Q versus the carrier wave number k . We find that due to the inhomogeneity effects, the domain of k in which $Q < 0$ (for which $PQ > 0$ and the modulational instability occurs) expands and the domain shifts towards lower values of k due to a reduction of the magnitude of Ω_0 . For example, for (i) $\Omega_0 = 0.8, \omega_J = 2.1\Omega_0, x = 0.5$, we have $Q_1 < 0 (> 0)$ in $0.6 \lesssim k < 0.624$ ($k \gtrsim 0.624$) (See the solid line of Fig. 3) (ii) $\Omega_0 = 0.8, \omega_J = 2.1\Omega_0, x = 1.5$, we have $Q_1 < 0 (> 0)$ in $0.85 \lesssim k < 0.94$ ($k \gtrsim 0.94$) (See the dashed line of Fig. 3), and (iii) $\Omega_0 = 0.5, \omega_J = 2.1\Omega_0, x = 1.5$, we have $Q_1 < 0 (> 0)$ in $0.39 \lesssim k < 0.41$ ($k \gtrsim 0.41$) (See the dotted line of Fig. 3). The other fixed parameter values are $c_s = 0.5$ and $\psi_0 = -0.5$.

In the case of $PQ > 0$ for which the modulational instability occurs, the instability growth rate (Γ) can be obtained from Eq. (35) for $K < K_c$ as

$$\Gamma = |P|K\sqrt{K_c^2 - K^2}, \quad (36)$$

where $K_c = \sqrt{2\eta_0 Q/P}$ is the critical wave number of perturbation, and the maximum growth rate, $\Gamma_{\max} = \eta_0|Q|$ is attained at $K = K_c/\sqrt{2}$.

Figure 4 displays the growth rate of instability [Eq. (36)] for different parameter values as in Fig. 2. We find that the instability growth rate can be enhanced and maximized by the effects of the magnetic field or density inhomogeneity. However, it can be reduced or minimized by reducing the angular frequency Ω_0 compared to the Jeans frequency.

C. Case III: $\omega_J > 2\Omega_0$, $k < k_J$

Here, we consider the most interesting case when $\omega_J > 2\Omega_0$, but $k < k_J$. From the analysis in Sec. III A, it is evident that the carrier wave frequency ω is purely imaginary (Jeans instability) and so are the coefficients P and Q of the NLS equation. Thus, assuming $P = iP_1$ and $Q = iQ_1$, Eq. (35) gives

$$\Omega = P_1K\sqrt{\frac{2\eta_0Q_1}{P_1} - K^2}, \quad (37)$$

where P_1 and Q_1 are reals, given by,

$$\begin{aligned} P_1 &= \frac{1}{2} \frac{\omega_J^2 - 4\Omega_0^2}{[c_s^2 + V_A^2(x)]^{1/2} (k_J^2 - k^2)^{3/2}}, \\ Q_1 &= -\frac{1}{2\gamma} \left[-\gamma^2 + \frac{1}{3} \frac{3\gamma^2 + c_s^2 k^2}{\omega_J^2 - 4\Omega_0^2} \right. \\ &\quad \left. \times (4\gamma^2 - 2k^2 - (\omega_J^2 - 4\Omega_0^2)) \right], \end{aligned} \quad (38)$$

with

$$\begin{aligned} \gamma &\equiv \Im\omega = \sqrt{[c_s^2 + V_A^2(x)](k_J^2 - k^2)} \\ &= \sqrt{[c_s^2 + V_A^2(x)]k^2 + \omega_J^2 - 4\Omega_0^2}. \end{aligned} \quad (39)$$

From Eq. (37), we find that the instability condition depends on the sign of the product P_1Q_1 and/or on the value of K smaller or larger than a critical value K_c . When $P_1Q_1 < 0$, Eq. (37) gives Ω purely imaginary for all values of K and so we have the modulational instability for all K , but with $k < k_J$. The corresponding growth rate of instability can be obtained by setting $\Omega = i\Gamma_1$ as

$$\Gamma_1 = |P_1|K\sqrt{2\eta_0\left|\frac{Q_1}{P_1}\right| + K^2}. \quad (40)$$

On the other hand, when $P_1Q_1 > 0$, the modulational instability occurs for $K > K_c$, where K_c is the critical wave number, given by,

$$K_c = \sqrt{2\eta_0\left|\frac{Q_1}{P_1}\right|}. \quad (41)$$

The corresponding instability growth rate is given by

$$\Gamma_2 = |P_1|K\sqrt{K^2 - 2\eta_0\left|\frac{Q_1}{P_1}\right|}. \quad (42)$$

However, the modulated wave is stable for $K < K_c$. The instability condition stated above is in contrast to the typical condition ($PQ > 0$, $K < K_c$) of modulational instability of wave envelopes in plasmas without self-gravity effects. Inspecting on the coefficients $P (= iP_1)$ and $Q (= iQ_1)$, we find that P_1 is always positive for $k < k_J$ and $\omega_J > 2\Omega_0$. From Fig. 5, we find that Q_1 can be both positive and negative in a finite domain of $k (< k_J)$. The domain for $Q_1 > 0$ in which the modulational instability occurs expands due to the effects of magnetic field or density inhomogeneity and shrinks due to reduction of the contribution from the Coriolis force compared to the self-gravitating force. For example, for (i) $\Omega_0 = 0.8$, $\omega_J = 2.1\Omega_0$, $x = 0.5$, we have $Q_1 < 0 (> 0)$ in $0 < k < 0.33$ ($0.33 \lesssim k \lesssim 0.594$) (See the solid line of Fig. 5) (ii) $\Omega_0 = 0.8$, $\omega_J = 2.1\Omega_0$, $x = 1.5$, we have $Q_1 < 0 (> 0)$ in $0 < k < 0.4$ ($0.4 \lesssim k \lesssim 0.842$) (See the dashed line of Fig. 5), and (iii) $\Omega_0 = 0.5$, $\omega_J = 2.1\Omega_0$, $x = 1.5$, we have $Q_1 < 0 (> 0)$ in $0 < k < 0.22$ ($0.22 \lesssim k \lesssim 0.386$) (See the dotted line of Fig. 5). The other fixed parameter values are $c_s = 0.5$ and $\psi_0 = -0.5$.

Figure 6 displays the growth rates Γ_1 and Γ_2 [Eqs. (40) and (42)] corresponding to $P_1Q_1 < 0$ and $P_1Q_1 > 0$ respectively. Evidently, we have a growing modulational instability without any cut-off at any value of K . The growth rate becomes higher the larger is the Jeans frequency compared to the angular velocity.

V. APPLICATIONS AND DISCUSSIONS

The solar corona is typically a complex system in the self-gravitating field of the Sun, and has been known to be an active medium for the dynamics and stability of magnetosonic waves, since one of the most important problems of coronal heating is associated with the wave [35]. Recent Solar Optical Telescope (SOT) observations of small-scale oscillations also indicate the existence of fast magnetosonic waves in solar prominence threads and pillars [36]. Past observations in the X-ray corona also reported slowly moving perturbations that can propagate with the speed 400 km/s during the first nine minutes of filament disruption [37]. Such a velocity seems to be close to the Alfvén speed of fast magnetosonic waves in a low- β plasma. The speed was, however, reduced to 190 km/s and 20 km/s after twenty minutes and four hours respectively. To explain this observation, one can assume that the fast magnetosonic waves originating from disrupted filaments can propagate as slowly moving magnetosonic wave envelopes through the modulational instability [27].

Typical solar plasma parameters are [35] (i) the number density of electrons/ions, $n \sim 10^9 \text{ cm}^{-3}$, (ii) the electron temperature, $T_e \sim 10^{-3} \text{ K}$, and (iii) the plasma $\beta \sim 0.2$ ($\beta \rightarrow 0$) at the magnetic field strength, $B_0 \sim 4 \text{ G}$

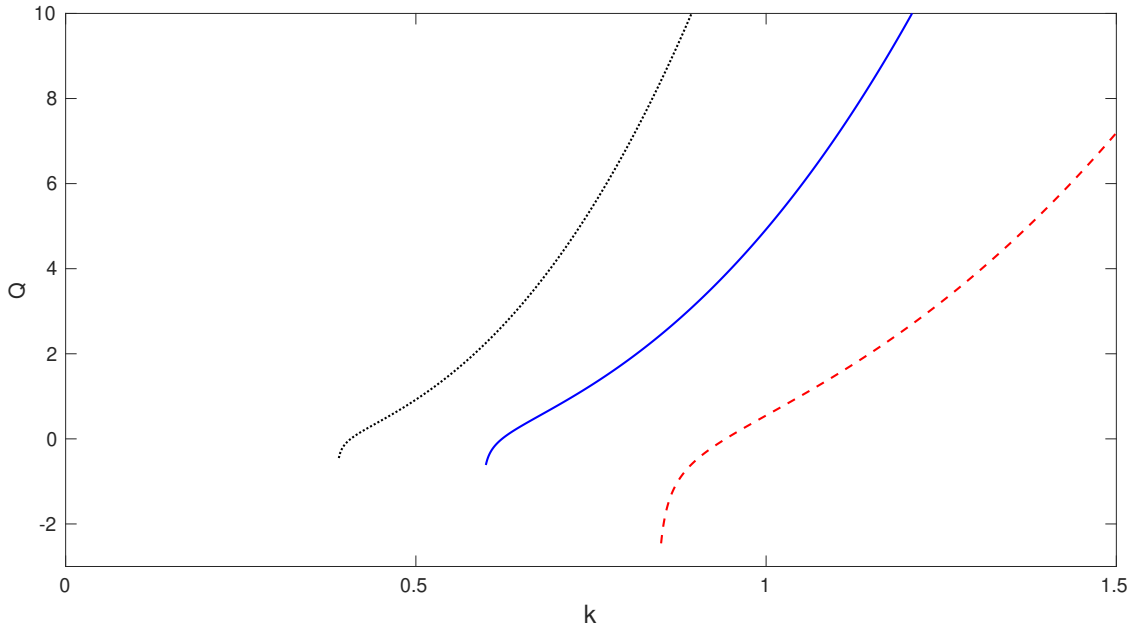


FIG. 3. Plot of Q [Eq. (30)] vs k is shown for Case II: $\omega_J > 2\Omega_0$, $k > k_J$. The fixed parameter values and different parameter values for the solid, dashed, and dotted lines are the same as for Fig. 2. Since $P < 0 \forall k$, the stable and unstable regions in k are corresponding to $Q > 0$ and $Q < 0$ respectively.

(40 G). For illustration purpose, we calculate the maximum growth rate in the case of $\omega_J > 2\Omega_0$, $k > k_J$ (Case II in Sec. IV B) at $B_0 = 4$ G as $\Gamma_{\max} \sim 0.0076$ (for $\eta_0 = 0.01$) such that the typical growth time can be estimated as $\tau_{\text{growth}} \sim 4$ s, i.e., faster than predicted before [27] and may be reasonable to explain the transition time (twenty minutes) from fast magnetosonic mode to slowly varying envelopes. The typical Jeans wavelength and the Alfvén velocity can be estimated as $\lambda_J \sim 2 \times 10^4$ m and $V_A \sim 3 \times 10^5$ m/s. We can also estimate the group velocity as $v_g \sim 5 \times 10^5$ m/s. These velocities are close to the observational velocity 190 km/s of slowly moving perturbations. The instability growth rate can be significantly high by the effects of the magnetic field and density inhomogeneities where the Alfvén velocity $V_A(x)$ gets reduced. Note that the above results are valid for low- β plasmas where the length scale of magnetic field inhomogeneity is much smaller than that of the density inhomogeneity and the wavelength associated with the fast carrier magnetosonic mode is small compared to the wavelength of the slow modulation along the magnetic field. On the other hand, the typical growth rate can be high having no cut-off at any wavelength of modulation, and the corresponding time scale can be low in the case when $\omega_J > 2\Omega_0$ and $k < k_J$ (Case III in Sec. IV B). However, to be consistent with the small perturbations, the admissible growth rate should be at a wavelength (of slow modulation) above its critical value.

It has been established that the fast magnetosonic mode can act as a candidate for coronal loop heating through the exchange of energy and momentum [35]. The

present theory of modulational instability should help predict the energy transfer rate of slowly varying magnetosonic envelopes in solar plasmas under the relative influences of the self-gravity force and the Coriolis force and the excitation of fast magnetosonic carrier modes at length scales below or above the Jeans critical length.

It is to be noted that in the case of plasmas with constant gravity, the gravity force, $\mathbf{g} = -\nabla\psi$ is to be replaced by $\mathbf{g} = (-g, 0, 0)$ and there will be no gravitational Poisson equation. Even if it is considered for the sake of clarity, it will result into the quasineutrality condition, already assumed for the derivation of the MHD equations. In this case, the term $-\omega_J^2$ in the dispersion equation (22) for the fast magnetosonic carrier waves will be replaced by igk , which will result into the real wave frequency, given by,

$$\omega_r^2 = [c_s^2 + V_A^2(x)] k^2 + 4\Omega_0^2 \quad (43)$$

and the instability growth rate, $\gamma = gk/\omega_r$. From the inhomogeneous equilibrium state one can obtain by the same assumption as for the fluid density in Sec. II A as $\rho_0(x) \approx \rho_0 + gx$. The coefficients of the group velocity dispersion (P) and the nonlinearity (Q) in the NLS equation will be complex, given by,

$$P = \frac{1}{2\omega^2} \left[(c_s^2 + V_A^2(x)) (\omega - v_g k) - \frac{1}{2} igv_g \right], \quad (44)$$

$$Q = \frac{1}{2\omega} \left(\omega^2 - \frac{\omega_1 \omega_2}{6\Omega_0^2 + igk} \right), \quad (45)$$

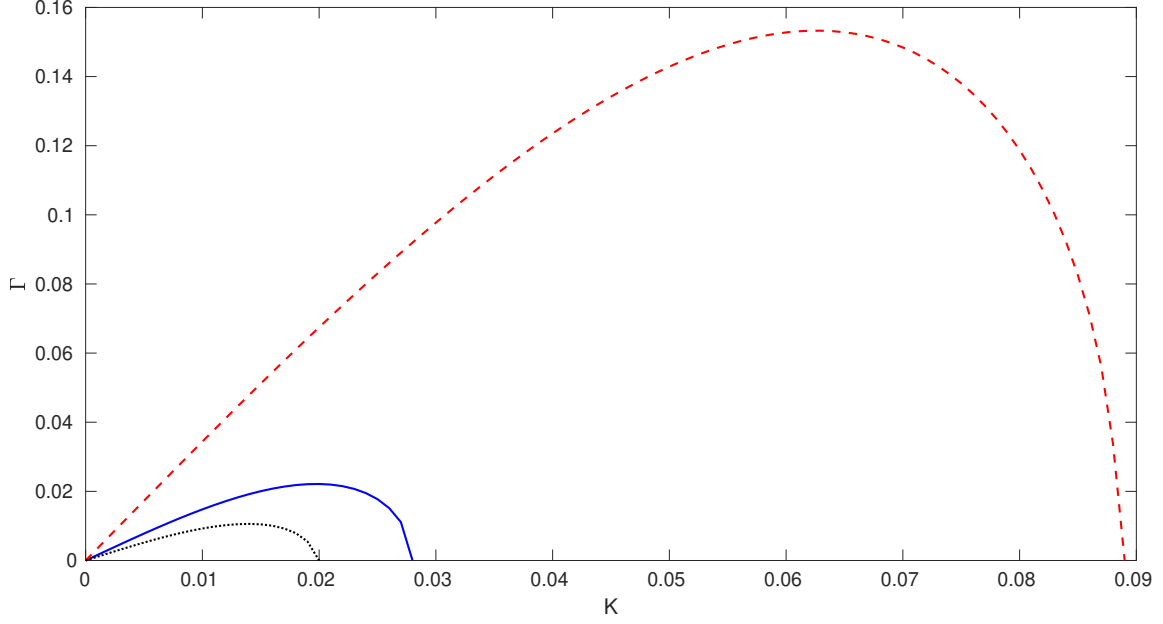


FIG. 4. The modulational instability ($PQ > 0$) growth rate Γ [Eq. (36)] is shown against the modulation wave number K of perturbation. The fixed parameter values and different parameter values for the solid, dashed, and dotted lines are the same as for Fig. 2.

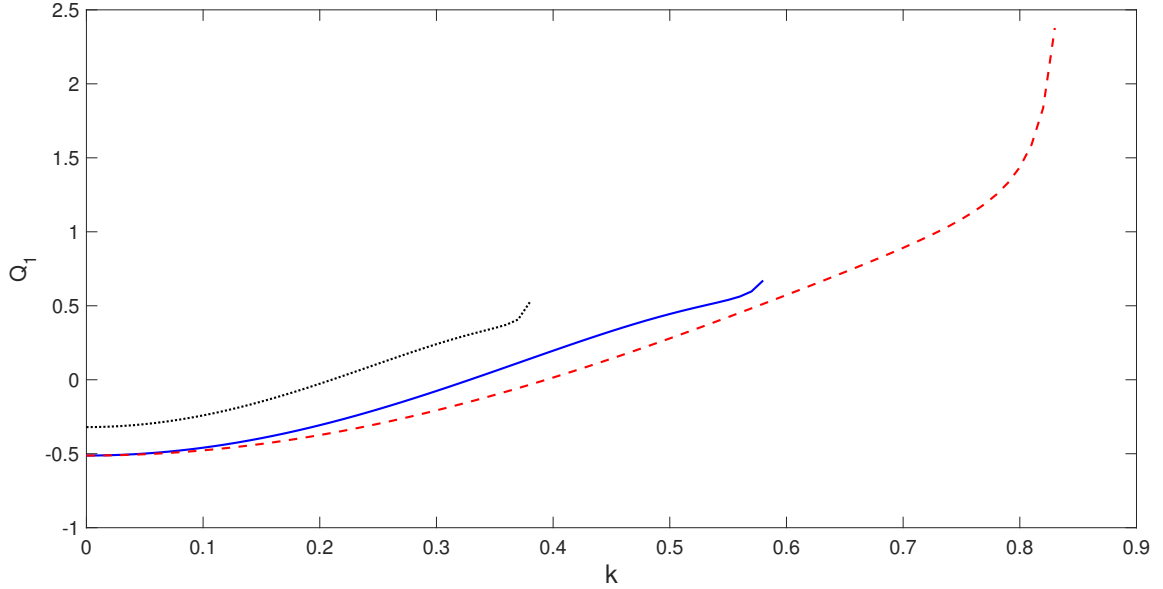


FIG. 5. Plot of Q_1 versus k is shown for Case III: $\omega_J > 2\Omega_0$, $k < k_J$. The fixed parameter values and different parameter values for the solid, dashed, and dotted lines are the same as for Fig. 2.

where $\omega_1 = (3V_A^2(x) + 2c_s^2)k^2 + 12\Omega_0^2 + 2igk$ and $\omega_2 = (3V_A^2(x) + 2c_s^2)k^2 + 6\Omega_0^2 + 2igk$. Consequently, instead of the purely growing instability as in Case III of Sec. IV C, we have the frequency up-shift (Ω_r) and the modulational

instability growth rate (Γ), given by,

$$\Omega_r = \frac{1}{\sqrt{2}} \left[-N + \sqrt{N^2 + 4M^2} \right]^{1/2}, \quad (46)$$

$$\Gamma = \frac{1}{\sqrt{2}} \left[N + \sqrt{N^2 + 4M^2} \right]^{1/2}, \quad (47)$$

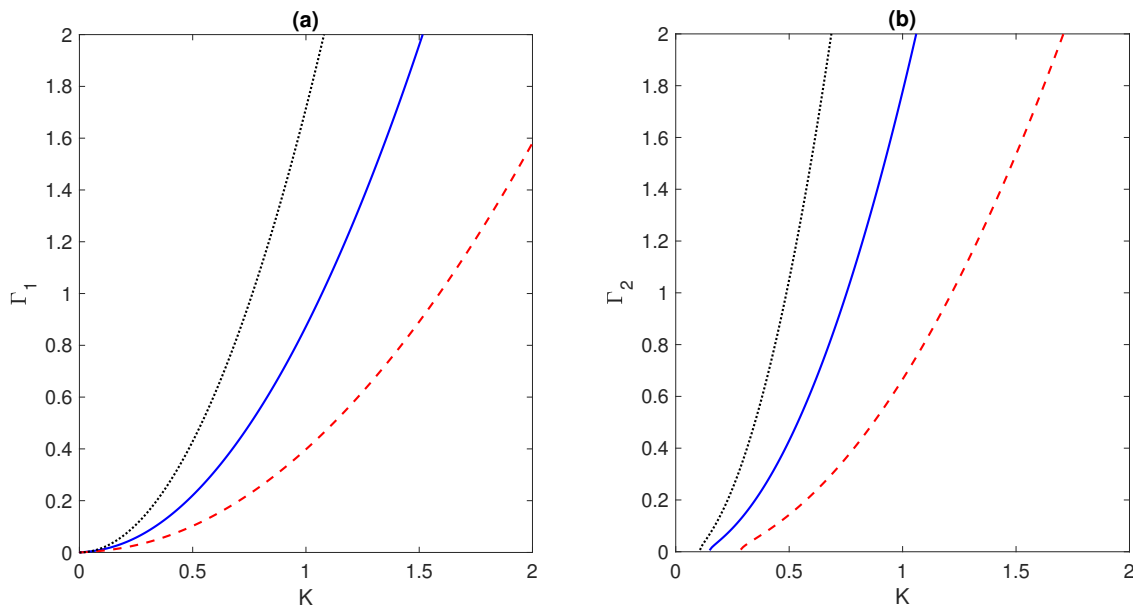


FIG. 6. The instability growth rates (a) Γ_1 [Eq. (40), when $P_1Q_1 < 0$] Γ_2 [Eq. (42), when $P_1Q_1 > 0$] are plotted against the modulation wave number K of perturbation. The fixed parameter values and different parameter values the solid, dashed, and dotted lines are the same as for Fig. 2.

where the expressions for M and N are

$$M = K^2 \{P_1P_2K^2 - \eta_0(P_2Q_1 + Q_2P_1)\}, \quad (48)$$

$$N = K^2 \{2\eta_0(P_1Q_1 + P_2Q_2) - (P_1^2 - P_2^2)K^2\}. \quad (49)$$

For brevity, we have presented the characteristics of Ω_r and Γ as shown in Fig. 7. It is found that both assume higher values at a reduced angular frequency Ω_0 (the dotted lines) and by the effects of the density inhomogeneity (the dashed lines). Also, the growth rate Γ is similar to Case III of Sec. IV C in self-gravitating plasmas, i.e., it grows with the wave number of modulation K without any cut-offs.

Thus, the instabilities of fast magnetosonic modes and the MI of slowly varying wave envelopes under the influences of self-gravity force and the constant gravity force are quite distinctive. While the Jeans critical wavelength appears above which the Jeans instability of fast carrier modes occurs and hence the MI of magnetosonic envelopes in self-gravitating fields, the fast modes appears to be unstable by the constant gravity force without any restriction of the wavelength unless the length at which the collective behaviors disappear. Furthermore, in contrast to plasmas under constant gravity, the stable Jeans mode in self-gravitating fields may give rise to the MI of slowly varying envelopes with a finite growth rate and cut-off at a finite wave number of modulation (See Case II in Sec. IV B).

VI. SUMMARY AND CONCLUSION

To summarize, we have studied the dispersion properties of fast magnetosonic waves and the modulation of slowly varying magnetosonic wave envelopes in inhomogeneous magnetoplasmas under the relative influence of the gravitational force and the Coriolis force due to rotating fluids. Using the multiple-scale reductive perturbation technique, we have derived the NLS equation for the evolution of slowly varying magnetosonic envelopes. It is found that the inhomogeneities in the background magnetic field and the fluid density favor the Jeans instability to occur in a larger domain of the carrier wave number (k) below the Jeans critical wave number (k_J). The latter is, however, defined when the self-gravity force dominates over the Coriolis force or the Jean frequency ω_J becomes larger than the increased angular frequency $2\Omega_0$. On the other hand, when the Coriolis force dominates over the self-gravity force or is dominated by the self-gravity force with $k > k_J$, the fast magnetosonic carrier mode is always stable. It is interesting to note that the MSW envelope, corresponding to the unstable carrier Jeans mode with $\omega_J > 2\Omega_0$ and $k < k_J$, is always unstable under the plane wave modulation having no cut-offs in the growth rates. However, the stable Jeans mode with $\omega_J > 2\Omega_0$ but $k > k_J$ can lead to modulational stability or instability with finite growth rates and cut-offs. Such an instability growth rate is enhanced by the effects of the magnetic field or density inhomogeneities. We have also discussed the possible applications of modulational instability in solar plasmas, such as those in the X-ray corona and solar prominence, and noted that the estimated Alfvén velocity of fast modes and the group

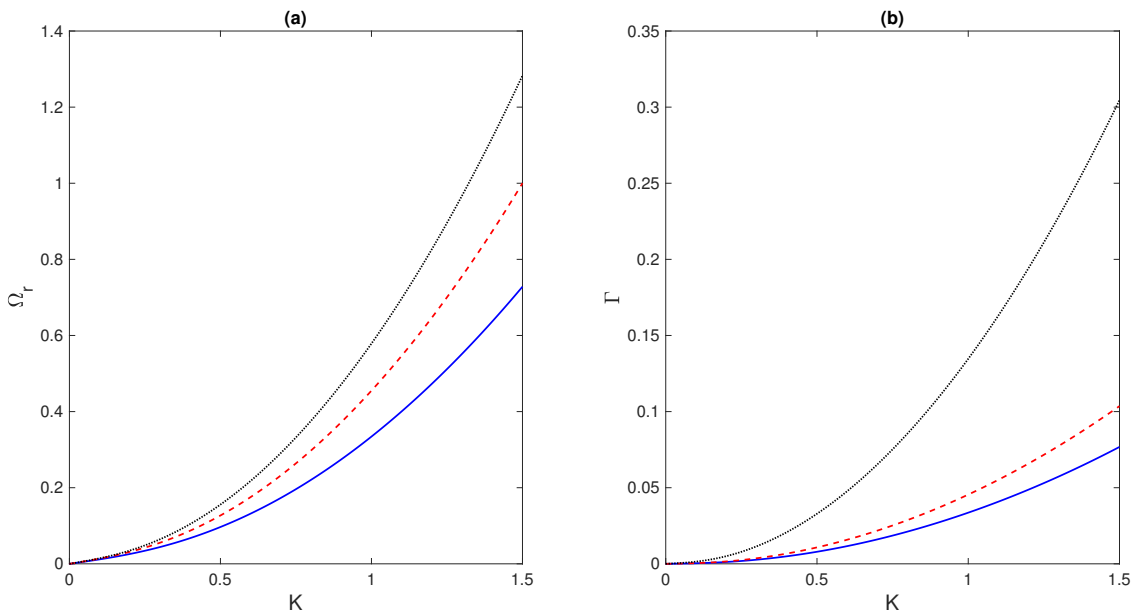


FIG. 7. The frequency shift [subplot (a), Eq. (46)] and the instability growth rate [subplot (b), Eq. (47)] are plotted against the modulation wave number K of perturbation. The solid, dashed, and dotted lines correspond to the parameter values as for Fig. 2. The other fixed parameter (normalized) values are $g = 0.5$, $c_s = 0.5$, and $k = 0.4$.

velocity of slowly varying envelopes are close to the observational values. Also, the estimated growth time is found to be reasonable to explain the transition time from the fast magnetosonic modes to slowly varying envelopes at the nonlinear stage.

As an illustration, we have also examined the influence of the constant gravity force instead of the self-gravitation. It is found that the fast carrier magnetosonic mode is always unstable, leading to a frequency up-shift of the frequency of modulation (instead of a purely unstable mode) and the instability growth rate having no cut-offs, similar to Case III of self-gravitating plasmas.

To conclude, since the fast magnetosonic modes can be a candidate for coronal loop heating in which the momentum and energy transfer occur, the theoretical results should help predict the growth time of slowly varying magnetosonic envelopes that can be transformed from the fast magnetosonic modes emanating from disrupted filaments in the X-ray corona through nonlinear interactions. The higher the growth rate shorter is the time scale for the instability. It is to be noted that the proposed coronal heating mechanism has been the collisionless Landau damping. The fast magnetosonic modes propagating parallel or perpendicular to the magnetic field cannot suffer collisionless damping, but may be damped due to viscosity effects [27]. However, it has been shown that modulational instability is the dominant mechanism for energy transfer in the coronal loops than the viscous damping [27]. The detailed investigation in this direction is beyond the scope of the present study. Accordingly, multi-dimensional propagation of magnetosonic waves in dissipative plasmas could be a project of future study.

ACKNOWLEDGMENTS

One of us, J. Turi, wishes to thank the Council of Scientific and Industrial Research (CSIR) for a Senior Research Fellowship (SRF) with reference number 09/202(0115)/2020-EMR-I. The authors also thank Sima Roy of the University of Engineering & Management, Kolkata, for rechecking the derivations of different expressions for the NLS equation.

AUTHOR DECLARATIONS

Conflict of Interest

The authors have no conflicts to disclose.

Author Contributions

J. Turi: Writing–draft, Methodology, Investigation, Formal analysis. **A. P. Misra:** Writing–draft, review & editing, Validation, Methodology, Investigation, Formal analysis, Conceptualization.

DATA AVAILABILITY STATEMENT

All data that support the findings of this study are included within the article (and any supplementary files).

N-TH ORDER REDUCED EQUATIONS

We apply the transformations [Eqs. (17) and (18)] and substitute the expansions [Eq. (19)] into Eqs. (5)-(9), to get the following set of reduced n-th order equations:

$$\begin{aligned}
 & -i\omega l B_l^{(n)} - \lambda \frac{\partial}{\partial \xi} B_l^{(n-1)} + \frac{\partial}{\partial \tau} B_l^{(n-2)} + ilk \left[B_0(x) v_{xl}^{(n)} + \sum_{n'=1}^{\infty} \sum_{l'=-\infty}^{+\infty} v_{xl-l'}^{(n-n')} B_{l'}^{(n')} \right] \\
 & + \frac{\partial B_0(x)}{\partial x} v_{xl}^{(n)} + B_0(x) \frac{\partial}{\partial \xi} v_{xl}^{(n-1)} + \sum_{n'=1}^{\infty} \sum_{l'=-\infty}^{+\infty} \frac{\partial}{\partial \xi} (v_{xl-l'}^{(n-n')} B_{l'}^{(n'-1)}) = 0
 \end{aligned} \tag{50}$$

$$\begin{aligned}
 & -i\omega l B_0(x) v_{xl}^{(n)} - \lambda B_0(x) \frac{\partial}{\partial \xi} v_{xl}^{(n-1)} + B_0(x) \frac{\partial}{\partial \tau} v_{xl}^{(n-2)} + \sum_{n'=1}^{\infty} \sum_{l'=-\infty}^{+\infty} \left[-i\omega l' B_{l-l'}^{(n-n')} v_{xl'}^{(n')} - \lambda B_{l-l'}^{(n-n')} \frac{\partial}{\partial \xi} v_{xl'}^{(n'-1)} \right. \\
 & + B_{l-l'}^{(n-n')} \frac{\partial}{\partial \tau} v_{xl'}^{(n'-2)} + il' k B_0(x) v_{xl-l'}^{(n-n')} v_{xl'}^{(n')} + B_0(x) v_{xl-l'}^{(n-n')} \frac{\partial}{\partial \xi} v_{xl'}^{(n'-1)} \left. \right] + \sum_{n',n''=1}^{\infty} \sum_{l',l''=-\infty}^{+\infty} \left[il'' k B_{l-l'}^{(n-n')} v_{xl-l''}^{(n'-n'')} v_{xl''}^{(n'')} \right. \\
 & \left. + B_{l-l'}^{(n-n')} v_{xl-l''}^{(n'-n'')} \frac{\partial}{\partial \xi} v_{xl''}^{(n''-1)} \right] + c_s^2 \left(\frac{\partial B_0(x)}{\partial x} ilk B_l^{(n)} + \frac{\partial}{\partial \xi} B_l^{(n-1)} \right) \\
 & + \left[ilk B_0(x) B_l^{(n)} + B_0(x) \frac{\partial}{\partial \xi} B_l^{(n-1)} + \sum_{n'=1}^{\infty} \sum_{l'=-\infty}^{+\infty} \left[il' k B_{l-l'}^{(n-n')} B_{l'}^{(n')} + B_{l-l'}^{(n-n')} \frac{\partial}{\partial \xi} B_{l'}^{(n'-1)} + B_0(x) \frac{\partial B_0(x)}{\partial x} + \frac{\partial B_0(x)}{\partial x} B_l^{(n)} \right] \right. \\
 & \left. + 2\Omega_0 \cos \lambda \left[B_0(x) v_{zl}^{(n)} + \sum_{n'=1}^{\infty} \sum_{l'=-\infty}^{+\infty} B_{l-l'}^{(n-n')} v_{zl'}^{(n')} \right] - 2\Omega_0 \sin \lambda \left[B_0(x) v_{yl}^{(n)} + \sum_{n'=1}^{\infty} \sum_{l'=-\infty}^{+\infty} B_{l-l'}^{(n-n')} v_{yl'}^{(n')} \right] \right. \\
 & \left. - \left[B_0(x) \frac{\partial \psi_0(x)}{\partial x} + \frac{\partial \psi_0(x)}{\partial x} B_l^{(n)} + ilk B_0(x) \psi_l^{(n)} + \sum_{n'=1}^{\infty} \sum_{l'=-\infty}^{+\infty} B_{l-l'}^{(n-n')} \frac{\partial}{\partial \xi} \psi_{l'}^{(n'-1)} + \sum_{n'=1}^{\infty} \sum_{l'=-\infty}^{+\infty} il' k B_{l-l'}^{(n-n')} \psi_{l'}^{(n')} \right. \right. \\
 & \left. \left. + B_0(x) \frac{\partial}{\partial \xi} \psi_l^{(n-1)} \right] = 0
 \end{aligned} \tag{51}$$

$$-i\omega l v_{yl}^{(n)} - \lambda \frac{\partial}{\partial \xi} v_{yl}^{(n-1)} + \frac{\partial}{\partial \tau} v_{yl}^{(n-2)} + \sum_{n'=1}^{\infty} \sum_{l'=-\infty}^{+\infty} \left[il' k v_{xl-l'}^{(n-n')} v_{yl'}^{(n')} + v_{xl-l'}^{(n-n')} \frac{\partial}{\partial \xi} v_{yl'}^{(n'-1)} \right] + 2\Omega_0 \sin \lambda v_{xl}^{(n)} = 0 \tag{52}$$

$$-i\omega l v_{zl}^{(n)} - \lambda \frac{\partial}{\partial \xi} v_{zl}^{(n-1)} + \frac{\partial}{\partial \tau} v_{zl}^{(n-2)} + \sum_{n'=1}^{\infty} \sum_{l'=-\infty}^{+\infty} \left[il' k v_{xl-l'}^{(n-n')} v_{zl'}^{(n')} + v_{xl-l'}^{(n-n')} \frac{\partial}{\partial \xi} v_{zl'}^{(n'-1)} \right] - 2\Omega_0 \cos \lambda v_{xl}^{(n)} = 0 \tag{53}$$

$$\frac{\partial^2 \psi_0(x)}{\partial x^2} - l^2 k^2 \psi_l^{(n)} + 2ilk \frac{\partial}{\partial \xi} \psi_l^{(n-1)} + \frac{\partial^2}{\partial \xi^2} \psi_l^{(n-2)} + \omega_j^2 B_0(x) + \omega_j^2 B_l^{(n)} = 0 \tag{54}$$

- [1] H. Alfvén, Existence of electromagnetic-hydrodynamic waves, *Nature* 150 (3805) (1942) 405–406.
 [2] A. Hannan, T. Hellsten, T. Johnson, Fast wave current drive scenarios for demo, *Nuclear Fusion* 53 (4) (2013)

043005.
 [3] K. Stasiewicz, P. Bellan, C. Chaston, C. Kletzing, R. Lysak, J. Maggs, O. Pokhotelov, C. Seyler, P. Shukla, L. Stenflo, et al., Small scale alfvénic structure in the

- aurora, *Space Science Reviews* 92 (2000) 423–533.
- [4] K. Stasiewicz, P. Shukla, G. Gustafsson, S. Buchert, B. Lavraud, B. Thidé, Z. Klos, Slow magnetosonic solitons detected by the cluster spacecraft, *Physical review letters* 90 (8) (2003) 085002.
- [5] K. Stasiewicz, Theory and observations of slow-mode solitons in space plasmas, *Physical review letters* 93 (12) (2004) 125004.
- [6] P. K. Shukla, L. Stenflo, R. Bingham, B. Eliasson, Non-linear effects associated with dispersive alfvén waves in plasmas, *Plasma physics and controlled fusion* 46 (12B) (2004) B349.
- [7] P. Shukla, B. Eliasson, L. Stenflo, Alfvénic shock waves in a collisional magnetoplasma, *Physics Letters A* 375 (24) (2011) 2371–2373.
- [8] K. Klein, G. Howes, J. TenBarge, S. Bale, C. Chen, C. Salem, Using synthetic spacecraft data to interpret compressible fluctuations in solar wind turbulence, *The Astrophysical Journal* 755 (2) (2012) 159.
- [9] J. Schmidt, L. Ofman, Slow magnetoacoustic wave oscillation of an expanding coronal loop, *The Astrophysical Journal* 739 (2) (2011) 75.
- [10] B. Rau, T. Tajima, Strongly nonlinear magnetosonic waves and ion acceleration, *Physics of Plasmas* 5 (10) (1998) 3575–3580.
- [11] M. Marklund, B. Eliasson, P. K. Shukla, Magnetosonic solitons in a fermionic quantum plasma, *Physical Review E* 76 (6) (2007) 067401.
- [12] F. Haas, S. Mahmood, Magnetosonic waves in a quantum plasma with arbitrary electron degeneracy, *Physical Review E* 97 (6) (2018) 063206.
- [13] W. Masood, R. Jahangir, B. Eliasson, M. Siddiq, A nonlinear model for magnetoacoustic waves in dense dissipative plasmas with degenerate electrons, *Physics of Plasmas* 21 (10) (2014).
- [14] S. Hussain, S. Mahmood, Korteweg-de vries burgers equation for magnetosonic wave in plasma, *Physics of Plasmas* 18 (5) (2011).
- [15] M. Salahuddin, H. Saleem, M. Saddiq, Ion-acoustic envelope solitons in electron-positron-ion plasmas, *Physical Review E* 66 (3) (2002) 036407.
- [16] S. Sultana, I. Kourakis, Electron-scale electrostatic solitary waves and shocks: the role of superthermal electrons, *The European Physical Journal D* 66 (2012) 1–12.
- [17] M. McKerr, I. Kourakis, F. Haas, Freak waves and electrostatic wavepacket modulation in a quantum electron-positron-ion plasma, *Plasma Physics and Controlled Fusion* 56 (3) (2014) 035007.
- [18] N. Chowdhury, A. Mannan, A. Mamun, Rogue waves in space dusty plasmas, *Physics of Plasmas* 24 (11) (2017).
- [19] M. S. Ruderman, Freak waves in laboratory and space plasmas: Freak waves in plasmas, *The European Physical Journal Special Topics* 185 (1) (2010) 57–66.
- [20] S. R. Habbal, E. Leer, T. E. Holzer, Heating of coronal loops by fast mode mhd waves, *Solar Physics* 64 (2) (1979) 287–301. doi:10.1007/BF00151440. URL <https://doi.org/10.1007/BF00151440>
- [21] S. Watanabe, Self-modulation of a nonlinear ion wave packet, *Journal of Plasma Physics* 17 (3) (1977) 487–501.
- [22] S. Sultana, I. Kourakis, Electrostatic solitary waves in the presence of excess superthermal electrons: modulational instability and envelope soliton modes, *Plasma Physics and Controlled Fusion* 53 (4) (2011) 045003.
- [23] S. Shalini, N. Saini, A. Misra, Modulation of ion-acoustic waves in a nonextensive plasma with two-temperature electrons, *Physics of Plasmas* 22 (9) (2015).
- [24] A. P. Misra, C. Bhowmik, Nonlinear wave modulation in a quantum magnetoplasma, *Physics of plasmas* 14 (1) (2007).
- [25] A. Bains, A. P. Misra, N. Saini, T. Gill, Modulational instability of ion-acoustic wave envelopes in magnetized quantum electron-positron-ion plasmas, *Physics of Plasmas* 17 (1) (2010).
- [26] W. Sahyouni, I. Zhelyazkov, P. Nenovski, Dark envelope solitons of fast magnetosonic surface waves in solar flux tubes, *Solar physics* 115 (1988) 17–32.
- [27] J.-I. Sakai, Modulational instability of fast magnetosonic waves in a solar plasma, *Solar Physics* 84 (1983) 109–118.
- [28] A. Misra, P. K. Shukla, Modulational instability of magnetosonic waves in a spin 1/2 quantum plasma, *Physics of Plasmas* 15 (5) (2008).
- [29] A. Panwar, C.-M. Ryu, Modulational instability and associated rogue structures of slow magnetosonic wave in hall magnetohydrodynamic plasmas, *Physics of Plasmas* 21 (6) (2014).
- [30] Y. Wang, X. Lü, B. Eliasson, Modulational instability of spin modified quantum magnetosonic waves in fermi-dirac-pauli plasmas, *Physics of Plasmas* 20 (11) (2013).
- [31] J. Turi, A. Misra, Magnetohydrodynamic instabilities in a self-gravitating rotating cosmic plasma, *Physica Scripta* 97 (12) (2022) 125603.
- [32] N. Asano, T. Taniuti, N. Yajima, Perturbation method for a nonlinear wave modulation. ii, *Journal of Mathematical Physics* 10 (11) (1969) 2020–2024.
- [33] J. H. Jeans, I. the stability of a spherical nebula, *Philosophical Transactions of the Royal Society of London. Series A, Containing Papers of a Mathematical or Physical Character* 199 (312-320) (1902) 1–53.
- [34] Y. H. Ichikawa, C. nonlinear wave modulation of electrostatic waves, *Progress of Theoretical Physics Supplement* 55 (1974) 212–232.
- [35] D. Y. Kolotkov, D. I. Zavershinskii, V. M. Nakariakov, The solar corona as an active medium for magnetoacoustic waves, *Plasma Physics and Controlled Fusion* 63 (12) (2021) 124008. doi:10.1088/1361-6587/ac36a5. URL <https://dx.doi.org/10.1088/1361-6587/ac36a5>
- [36] L. Ofman, T. A. Kucera, C. R. DeVore, Nonlinear fast magnetosonic waves in solar prominence pillars, *The Astrophysical Journal* 944 (2) (2023) 210. doi:10.3847/1538-4357/acb13b. URL <https://dx.doi.org/10.3847/1538-4357/acb13b>
- [37] D. M. Rust, Z. Švestka, Slowly moving disturbances in the x-ray corona, *Solar Physics* 63 (2) (1979) 279–295. doi:10.1007/BF00174535. URL <https://doi.org/10.1007/BF00174535>